Electrical Power and Energy Systems 54 (2014) 325–333

Contents lists available at ScienceDirect

Electrical Power and Energy Systems

journal homepage: www.elsevier.com/locate/ijepes

A new approach for optimal sizing of battery energy storage system for primary frequency control of islanded Microgrid

Mohammad Reza Aghamohammadi *, Hajar Abdolahinia

Department of Electrical Engineering, Power and Water University of Technology, Tehran, Iran

ARTICLE INFO

Article history:
Received 16 September 2012
Received in revised form 25 March 2013
Accepted 13 July 2013

Keywords:
Microgrid
Battery energy storage system (BESS)
Overloading characteristic
Microsources
Primary frequency control

ABSTRACT

This paper presents a method for determining optimal size of a battery energy storage system (BESS) for primary frequency control of a Microgrid. A Microgrid is assumed to be portion of a low voltage distribution feeder including sources such as microturbine, diesel generator, fuel cell and photovoltaic system with slow response for frequency control. A BESS due to its very fast dynamic response can play an important role in restoring balance between supply and demand. In this paper, overloading capacity of the BESS is employed for fast handling of the primary frequency control of a MG. To achieve this purpose, by considering overloading characteristics and limitations of the state of charge (SOC) of battery, a control scheme of dc/ac converter for the BESS is developed. Based on this scheme, overloading capacity of the BESS and its permissible duration for participating in primary frequency control is determined. Simulation studies are carried out using PSCAD/EMTDC software package to evaluate the performance of the proposed control scheme.

1. Introduction

Due to the increased demand for energy and environmental benefits of the renewable distributed generation (DG), DG sources such as fuel cells, wind turbine and photovoltaic arrays have a large utilization nowadays [1]. The increase in DG penetration depth and the presence of multiple DG units in electrical proximity to one another have brought about the concept of Microgrid (MG) [2,3]. A MG may consist of multiple distributed energy resources (DERs), customers, energy storage units and can be defined as a small electric power system being able to operate physically islanded or interconnected with the utility girds [4,5]. In the interconnected mode, the frequency and the voltage of the MG are controlled and maintained within a tight range by the main grid [6,7]. In the islanded mode, a MG mainly suffers from load-generation unbalance especially at the moment of disconnection and consequently its frequency may undergo rapid change due to the low inertia and small time constants of microsources present in the MG. Therefore, in the islanded mode primary frequency control is a critical issue which requires sufficient and fast reserve. A MG without adequate reserve may be under the risk of blackout [8]. Primary frequency control appears as a vital task for controlling and stabilizing MG during islanded operation [6,7,9].

For handling frequency problem of a MG, energy storage devices such as batteries, sodium–sulfur (NaS) batteries, flywheel energy storage (FES), super-capacitor, superconducting magnetic energy storage (SMES) and finally load-shedding are the key to guarantee the frequency control and smooth transition of MG into islanded mode [10,5]. In a MG, the energy storage devices with fast response play the role of the spinning reserve in the conventional power systems for preserving the balance between supply and demand especially during islanded operation [11].

Since renewable energy resources (RES) are naturally intermittent so, an energy storage system (ESS) is required to optimize their energy utilization [12–14]. The main role of ESS in a MG is to maintain stability, facilitate integration of the renewable energy and improving power quality. Fast response ESS can effectively damp electromechanical oscillations in power systems because they can provide storage capacity in addition to the kinetic energy of generators with the ability for sharing sudden changes in power requirement [15]. In [16], a cooperative control strategy for microsources and ESS during island operation is presented in which the ESS is responsible for the primary control of frequency and voltage, while the secondary control of MG management system returns the power output of the ESS to zero.

Battery energy storage system (BESS) is composed of static elements and has a very fast dynamic response compared to typical generators or other energy storage devices [17]. Battery energy storage systems (BESS) can cover a wide spectrum of applications ranging from short-term power quality support to long-term energy management [18]. The BESS technologies with fast response is able to perform multitask functions (e.g., load leveling, peak shaving, spinning reserve, black-start capability, uninterruptible power

* Corresponding author. Tel.: +98 (21)77312176; fax: +98 (21)73932591.
E-mail address: Aghamohammadi@pwut.ac.ir (M.R. Aghamohammadi).

0142-0615/$ - see front matter © 2013 Elsevier Ltd. All rights reserved.
http://dx.doi.org/10.1016/j.ijepes.2013.07.005

supply (UPS), flicker compensation, voltage sag correction, and area regulation) with the same device [19,20]. In fact, the future of the BESS certainly lies into multitasking, where a single modular and flexible unit can do peak shaving, load leveling, frequency control, load management, and so on [18]. Even if frequency control is not the primary task of a BESS, it is still economically attractive to assign a certain battery reserve to perform this particular task [18]. In [21], a dynamic model of BESS is derived for stability study of a large-scale power system and attempting to damp torsional oscillations of turbo generator.

In recent years, several BESS have been mainly installed worldwide for load leveling and peak shaving [18]. The BESS can satisfy the technical requirements for primary frequency control by absorbing power from the grid and injecting power to the grid during high and low frequency excursions respectively with respect to the nominal set point. Additionally, since the BESS is composed only of static elements, it has a very fast dynamic response compared to typical generators or other storage devices [18,17]. The great potential of BESS for frequency regulation has been demonstrated in [19]. The effect of BESS on the load–frequency control of an isolated power system is presented in [22] by promising improvement. Concerning investment cost for battery storage technologies, determination of optimal capacity for BESS for long term energy management performance is very important. In [23], an optimization method for dimensioning BESS for primary frequency control using a control algorithm based on the fixed SOC is developed for large interconnected power systems. In [24], for primary frequency control of an isolated power system an incremental model of the BESS has been implemented into the load–frequency control with improved performance. In [18], a method for optimal sizing and operation of BESS for use as spinning reserve in a small isolated power system is presented. The methods dealt with optimal sizing of BESS for frequency control have mainly considered the nominal capacity of BESS for primary frequency control.

In this paper, concerning overloading characteristics of BESS including overloading capacity and permissible overloading duration, a new algorithm is proposed for optimal sizing of the BESS for fast participating in primary frequency control of isolated MG. In fact, compared to the long term energy management performance of BESS, primary frequency control needs fast release of a relatively little energy which can be achieved by overloading characteristic of BESS.

For this purpose a control scheme is developed to implement overloading characteristics of BESS into primary frequency control. The energy exchange of the BESS during primary frequency control is not so much to violate the limits of the state of charge (SOC). Therefore, in the proposed approach, SOC limit violation is not so critical. However, in the proposed control scheme, limitations of the SOC of the BESS is considered. By using the simple and common method of column counting, the SOC is taken into account. Implementing the overloading characteristic of the BESS into primary frequency control will provide a chance for utilizing a BESS with very small size for restoring a relatively large unbalance power in a MG.

2. Study system

Fig. 1 shows single line diagram of the MG used for simulation studies. It consists of a 0.4 kV distribution feeder connected to a 20 kV distribution network through a 400 kV A transformer. The system structure and parameters are taken from the CIGRE low voltage distribution benchmark system [9]. The total installed capacity of the microsources is 79 kW. It consists of (1) a split-shaft microturbine (MT) with voltage-power ratings of 0.4 kV and 31.1 kV A equipped with an excitation system of the type of IEEE standard AC5A, (2) a diesel generator (DE) with voltage-power ratings of 0.4 kV and 31.1 kV A equipped with excitation system of the type of IEEE standard AC1A and governor control system, (3) a solid oxide fuel cell (SOFC) of 10 kW, (4) two photovoltaic arrays rating 10 and 3 kW respectively (PV), and (5) a BESS which is dedicated for primary frequency control and its capacity is supposed to be determined for this task. The split-shaft microturbine is based on the model of GAST turbine-governor presented in [25]. The diesel generator model used in the simulation is based on the model in the PSCAD/EMTDC software package used in [26]. The SOFC model is taken from the model used in [25]. Model description for photovoltaic array can be found in [16]. The BESS consists of a battery modeled as constant dc voltage source indirectly connected to the grid through power electronic convertor. The details of the BESS converter are given in the next chapters. As shown in Fig. 1, the microturbine and diesel generator are connected directly to the MG and fuel cell, photovoltaics and BESS are connected through power electronics convertors. The system and all microsources are properly modeled within PSCAD/EMTDC software.

3. Frequency and voltage control of MG

In the grid-connected mode, the voltage and frequency of MG are controlled by the main grid. However, in the islanded mode, its frequency and voltage may change rapidly due to the low inertia and small time constants of microsources. For proper operation of islanded MG, developing suitable control strategy is very important in order to maintain its frequency and voltage. If multiple microsources participate in the frequency and voltage regulation, frequency-droop and voltage-droop control strategies can be used to share power among microsources.

In this paper, BESS is considered as the main regulating unit for stable operation of a MG in the islanded mode. In fact, BESS due to its very fast dynamic response performs as a spinning reserve for primary frequency control. After stabilizing frequency of MG in the initial step of the primary control, active power-sharing among dispatchable microsources (microturbine, diesel generator and SOFC) is carried out based on their droop mechanism using Eq. (1) [27,28].

$$R_1 \times \Delta P_1 = R_2 \times \Delta P_2 = \ldots = cte \tag{1}$$

where ΔP_i and R_i are active power variation and regulating droop of the ith microsource, respectively. Eq. (2) governs frequency change of the MG following a disturbance.

$$\frac{df}{dt} = \frac{f_0}{2\sum_i H_i}\left(\sum_i P_{G_i} - \sum_i P_{L_i}\right) \tag{2}$$

where $\sum H_i$ is the sum of the inertia constants of all rotating machines. It is noteworthy that voltage of MG is controlled by the excitation systems of synchronous generators due to their fast responses. The process of the frequency control of MG is schematically illustrated in Fig. 2.

4. The proposed control scheme of BESS

The proposed control scheme of BESS is mainly based on the utilization of overloading capacity of the battery, including overloading capacity and permissible duration, for short term primary frequency control. Since the energy exchange of BESS during primary frequency control is low with respect to the energy excursion during long term energy management, the limit violation of SOC is not critical. However, in the proposed control scheme limitations

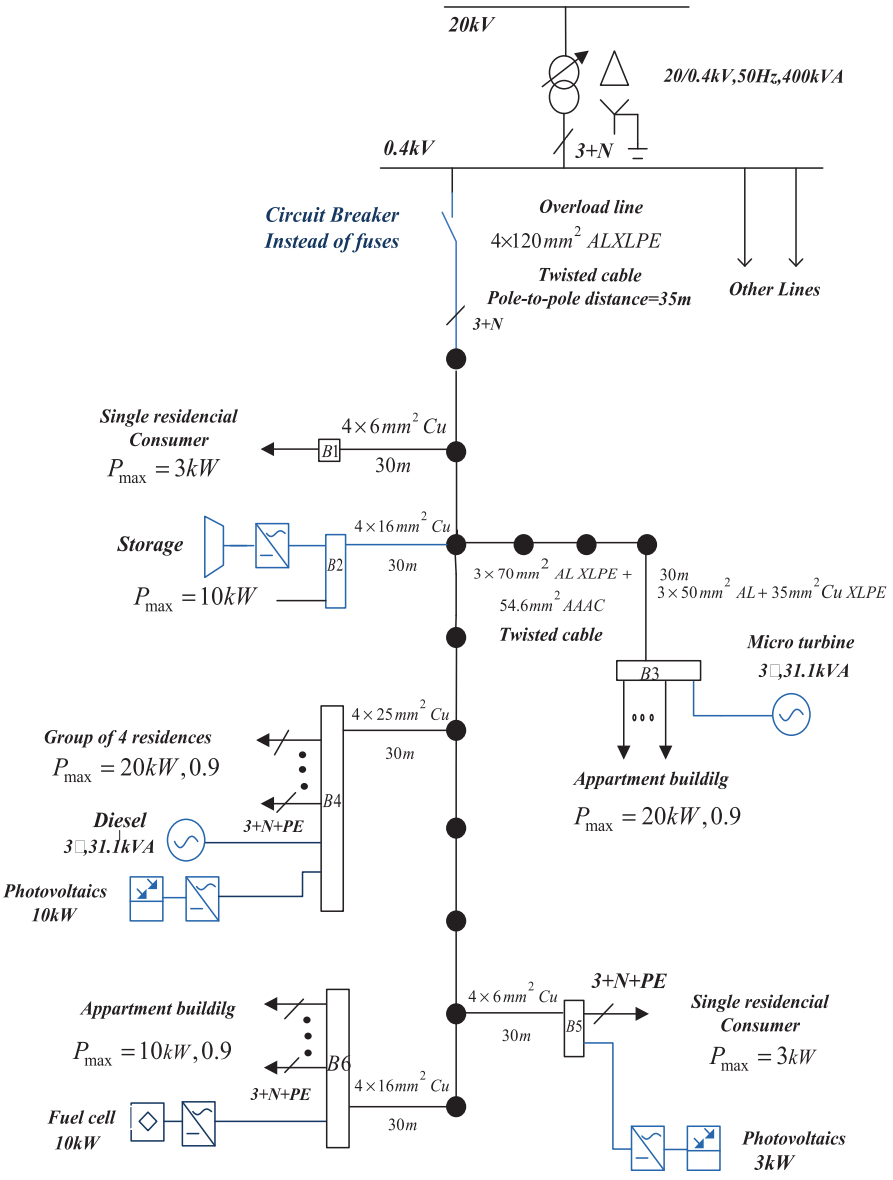

Fig. 1. Schematic diagram of the study system.

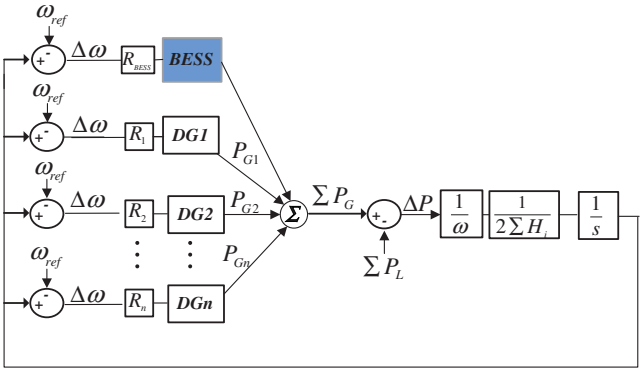

Fig. 2. The process of the frequency control of the MG.

of the SOC of BESS is considered and by using the simple and common method of coulomb counting.

During grid-connected mode, since there are references for frequency and voltage control, all microsources operate in PQ mode injecting specified active and reactive powers. However, in the islanded mode, since MG loses its frequency and voltage references, providing a reference for frequency and voltage control by BESS play an important role in stabilizing MG.

In this paper, the BESS is modeled as voltage source inverter (VSI) to handle sudden changes in frequency and voltage. Since the control capability of the BESS is determined by its available capacity for discharge and charge, therefore, after completing each task of frequency control, its power output should be brought back to zero by power sharing among other microsources. By this way it can be assured that the BESS is always ready to provide maximum spinning reserve (discharge/charge) to the MG. The conceptual model of the proposed control scheme for BESS is illustrated in Fig. 3.

The battery controller shown in Fig. 3 consists of current reference generation and current controller as illustrated in Fig. 4. The current reference generation determines d–q reference currents ($I_{d\text{-}ref}$, $I_{q\text{-}ref}$) based on the desired value of frequency and voltage and instantaneous values of active and reactive powers. The current controller shown in Fig. 5 generates d–q voltage references ($V_{d\text{-}ref}$, $V_{q\text{-}ref}$) using errors between d–q current references ($I_{d\text{-}ref}$,

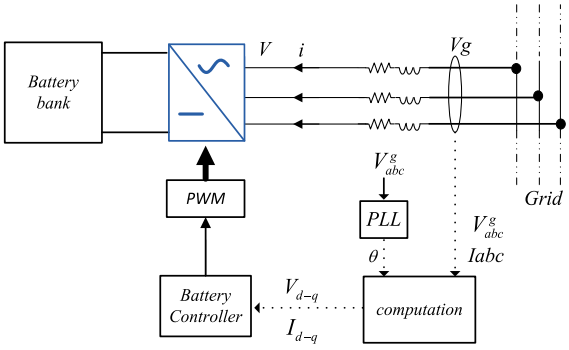

Fig. 3. Conceptual model of the proposed control scheme for the BESS.

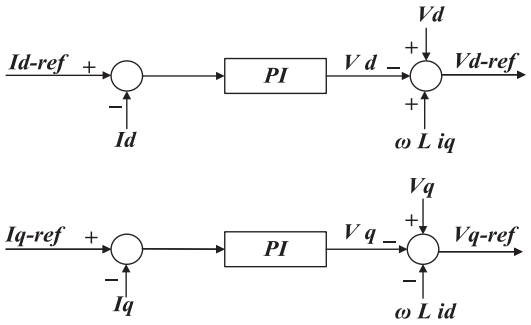

Fig. 5. Block diagram representation of current controller of the BESS.

$I_{q\text{-}ref}$). and the measured d–q current (I_d, I_q). Finally, through a transformation from d–q to abc, the three-phase reference voltage signals for the PWM are determined.

Fig. 5 shows block diagram of the current controller including two PI controllers for controlling the d–q currents.

Fig. 6 shows block diagram of the current reference generation including reference signals of SOC-*ref*, Q-*ref*, f-*ref* and V-*ref* for controlling SOC, reactive power, frequency and voltage of the BESS respectively. *P*, *Q*, *f* and *V* are the measured values for the real power, reactive power, frequency and voltage of the grid calculated by the computation block shown in Fig. 3.

SOC is the instantaneous value of the state of charge calculated by the state of charge estimator. As shown in Fig. 6, in grid-connected mode, the Q-ref value is set to zero and the BESS is charged up to SOC-ref. When islanding occurred, in order to avoid frequency and voltage fluctuation and to ensure balance between supply and demand, the BESS changes from charge mode to frequency and voltage control mode. In the proposed control scheme, as it is mentioned although the usage of SOC in the regime of primary frequency control is not so much to violate its limitation, but in order to consider SOC limitations, two new blocks for estimating SOC and state of overloading of battery are added to the dc/ac converter of the BESS. As mentioned, in the grid-connected mode the BESS is charged up to SOC-ref. In the islanded mode, in order to preserve a charge and discharge capability for the battery, the set point of the SOC-ref is set to a value smaller than 100%. For example, with SOC-ref = 60%, battery is able to exchange 40% of its capacity by charging and discharging until 100% and 20% respectively.

As it is mentioned since the usage of SOC in the regime of primary frequency control is not so much to violate its limitation, therefore, evaluation of SOC does not need to be more accurate and for this reason it can be estimated based on the simple and common method of coulomb counting by Eq. (3) [29–31].

$$\mathrm{SOC}(t)\% = \left(\mathrm{SOC}(t_0) - \left(\frac{\int_{t_0}^{t} i_{bat}(t)dt}{Q_N}\right)\right) \times 100 \tag{3}$$

where $\mathrm{SOC}(t_0)$ is the state of charge of the battery at t_0 which is taken as reference value for coulomb counting. In this approach, in accordance to the reference value 60% for SOC at the normal state, the value of $\mathrm{SOC}(t_0)$ can be re-calibrated at the 60% on a regular basis by resetting the SOC to 60% when it is not active for primary frequency control.

Q_N is battery rated capacity (Ah), and i_{bat} is discharge (+) or charging (−) current of battery. In order to protect the BESS, when its SOC get smaller than 20% or bigger than 100%, the BESS is taken out and its power output set to zero.

The efficiency of a battery is mainly related to its performance for long term energy production mode, while the proposed approach is mainly concerned with the short term overloading performance of BESS for primary frequency control so, the efficiency of battery in this regime is not concerned and considered as unity.

5. Overloading characteristic of battery

The overloading characteristics of battery including overloading capacity and its permissible duration are important features which dominate BESS capability for frequency control of MG in the islanded mode. In this paper, the terminal voltage of battery is assumed constant so, the overload capacity can be defined in term of its nominal capacity (V Ah). Permissible duration for overloading is inversely dependent on the overloading coefficient. The technical data concerning relationship between overloading coefficient and

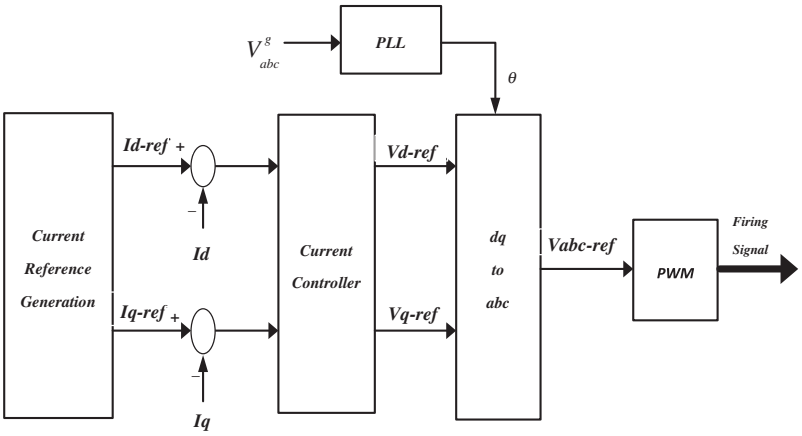

Fig. 4. Block diagram of battery controller of the BESS.

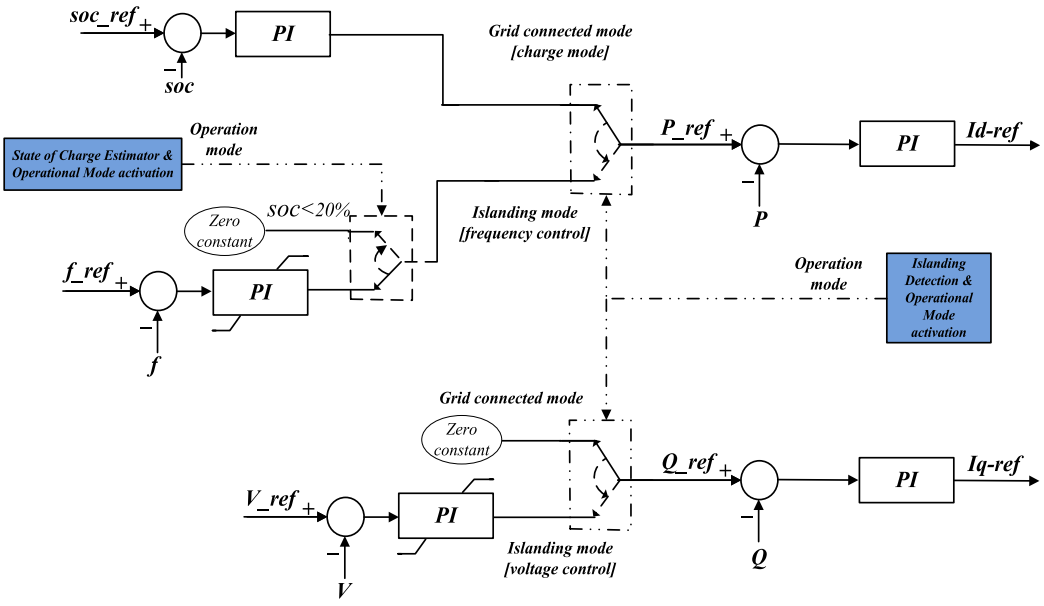

Fig. 6. The proposed block diagram for current reference generation of dc/ac converter of the BESS.

permissible duration are provided by the battery manufacturer. Based on these data, relationship between coefficient and permissible duration of overloading of the BESS in the charging mode can be numerically represented by the following equation:

$$T_{ov}^{ch} = \begin{cases} t_1^{ch} & if \quad P_{ov} \leqslant k_1^{ch} \\ \vdots & \vdots \\ t_i^{ch} & if \quad P_{ov} \leqslant k_i^{ch} \\ \vdots & \vdots \\ t_n^{ch} & if \quad P_{ov} \leqslant k_n^{ch} \end{cases} \tag{4}$$

where T_{ov}^{ch} is the permissible duration for overloading in charging mode (s), P_{ov} the overloading coefficient of battery ($P_{overloading}/P_{nom}$), k_i^{ch} the permissible overloading coefficient defined by manufacture where, $k_1^{ch} > \cdots > k_i^{ch} > \cdots > k_n^{ch}$, and t_i^{ch} is the permissible overloading duration corresponding to k_i^{ch} where, $t_1^{ch} < \cdots < t_i^{ch} < \cdots < t_n^{ch}$

As it can be seen, permissible overloading duration t_i^{ch} can be defined by the manufacturer with respect to the permissible overloading coefficient k_i^{ch} in a multistage overloading. According to Eq. (4), overloading of battery by coefficient k_i^{ch} means that it can tolerate this overloading by permissible duration t_i^{ch}. Permissible duration has an inverse relationship with the coefficient of overloading k_i^{ch} such that as the overloading coefficient becomes larger, the permissible duration gets smaller. Adequate overloading coefficient is determined by the frequency deviation.

Similarly, for the discharging mode the same relationship as Eq. (4) can be derived by the following equation:

$$T_{ov}^{dch} = \begin{cases} t_1^{dch} & if \quad P_{ov} \leqslant k_1^{dch} \\ \vdots & \vdots \\ t_i^{dch} & if \quad P_{ov} \leqslant k_i^{dch} \\ \vdots & \vdots \\ t_n^{dch} & if \quad P_{ov} \leqslant k_n^{dch} \end{cases} \tag{5}$$

where T_{ov}^{dch}, P_{ov}, k_i^{dch} and t_i^{dch} are overloading duration (s), overloading coefficient, permissible overloading coefficient and permissible duration respectively where $k_1^{dch} > \cdots > k_i^{dch} > \cdots > k_n^{dch}$ and $t_1^{dch} < \cdots < t_i^{dch} < \cdots < t_n^{dch}$.

For protecting the battery against overloading, a tolerating overload block (TOB) is proposed and added to the control scheme of the BESS. TOB works according to Eqs. (4) and (5). In the case of an overloading, the TOB measures overloading duration (t^{ov}) and if it exceeds the corresponding permissible duration ($t_{ov} > T_{ov}^{ch}$, (T_{ov}^{dch}), then it gives a command for switching off the battery with zero output.

6. Optimal sizing of BESS capacity

In the interconnected mode of MG, the balance between supply and demand is supported by the main grid without any need to ESS while, during islanded mode operation power balancing between supply and demand requires special strategy. In the islanded mode, in the case of occurrence of an unbalance between supply and demand powers, due to slow response and small inertia of microsources, frequency undergoes large excursion threatening system stability. In such situation, BESS with fast response can play an important role in the primary frequency control for balancing supply and demand in the initial stage. Therefore, BESS contribution for frequency control should be regarded for a short time immediately after occurrence of islanding or other disturbances. In this regard, due to short time contribution of BESS, its overloading characteristics can play an important role for its optimal sizing. In this paper, for minimizing BESS cost which is determined by its nominal power rating, the required power for primary frequency control is provided by overloading capacity of BESS instead of its nominal power. In other words, based on Eqs. (4) and (5), overloading characteristics of BESS can provide an output power bigger than its rated power up to several order. In this paper, considering overloading characteristics of BESS, a new approach for optimal sizing of its battery for primary frequency control is developed. In this approach, overloaded output power of BESS should be able to capture maximum mismatch power which can occur between supply and demand (e.g. at the moment of islanding). Maximum mismatch power of MG can be determined based on the average statistical exchange power between main grid and MG which can be in the form of either shortage or surplus of genera-

tion. Therefore, the required overloaded output power of the BESS ($P_{BESS}^{overload}$) is determined by the maximum mismatch power of MG as in the following equation:

$$P_{BESS}^{overload} = P_{mis}^{max} \tag{6}$$

where P_{mis}^{max} is the maximum mismatch power which can occur in the MG.

Islanding with surplus or shortage of generation require charging or discharging performance of the BESS respectively. Since battery performance for charge and discharge is different so, power overloading of the BESS for each situation should be determined separately and the bigger one is adopted for sizing capacity of the BESS. The process of the proposed algorithm for optimal sizing of the BESS for frequency control of MG is shown in Fig. 7 and described as follows.

Step 1: Define the maximum surplus power $P_{surplus}^{max}$ and shortage power $P_{shortage}^{max}$ based on the statistical exchange power between MG and the main gird and set to $P_{BESS}^{overload}$.
Step 2: First, the maximum permissible overloading coefficients for charge and discharge (k_1^{ch}, k_1^{dch}) are adopted for power sizing of the BESS. By using Eqs. (4) and (5) corresponding permissible durations of charge/discharge overloading (t_i^{ch}, t_i^{dch}) are evaluated.
Step 3: Based on the surplus and shortage power defined in step (1) and adopted overloading coefficients, the nominal power of the battery corresponding to charge and discharge situation are evaluated respectively as follows.

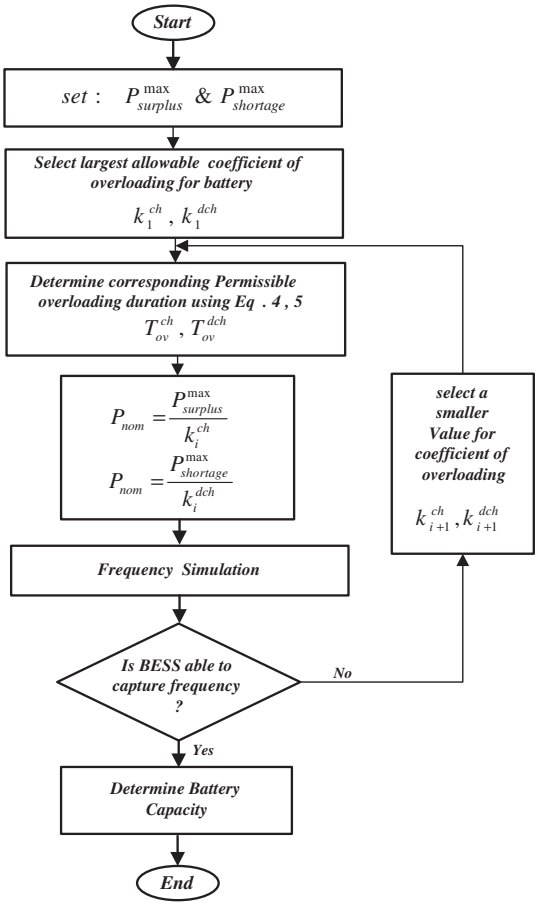

Fig. 7. Process of the optimal sizing of the BESS.

$$P_{nom}^{ch} = \frac{P_{surplus}^{max}}{K_i^{ch}} \tag{7}$$

$$P_{nom}^{dch} = \frac{P_{shortage}^{max}}{K_i^{dch}} \tag{8}$$

where P_{nom}^{ch} and P_{nom}^{dch} are nominal power (kW) of BESS obtained based on the surplus and shortage situations and K_i^{ch} and K_i^{dch} are permissible overloading coefficients of BESS at charge and discharge situations respectively.

Step 4: After determining nominal power and permissible overloading duration of the BESS, time domain frequency simulations of the isolated MG for the corresponding mismatch powers are carried out to evaluate the response of the designed BESS for primary frequency control of MG.

In fact permissible overloading duration of the BESS is the time duration which BESS can tolerate overloading for keeping power balance in the MG until other microsources change their output for capturing mismatch power.

If it is found that the permissible overloading duration of the BESS is sufficient for capturing mismatch power and keeping power balance for stabilizing frequency, the process will be ended, otherwise at the next step (5) a longer permissible overloading duration should be examined by adopting a smaller overloading coefficient.

Step 5: From Eqs. (4) and (5) the next smaller overloading coefficients (k_i^{ch} or k_i^{dch}) with longer corresponding permissible durations (t_i^{ch}, t_i^{dch}) are adopted and the process will be repeated again from step 3.

The process will be carried out until the overloading coefficient and its corresponding permissible duration are able to capture mismatch power and stabilizing frequency excursion of the MG. At the end of the process, the nominal power of the BESS is determined by Eqs. (7) and (8) for both surplus and shortage situations and the biggest one is adopted as the final power rating of the BESS.

7. Simulation studies

To demonstrate the capability of the proposed approach, it is applied on the study system shown in Fig. 1 for designing a proper BESS for primary frequency control. Load, generation and surplus/shortage mismatch powers of the MG for the critical scenarios of uncontrolled islanding which are extracted based on the history of the statistical exchange power of the MG with the main grid are given in Table 1. The disturbance is sudden disconnection of the MG from the main grid under two surplus and shortage scenarios shown in Table 1.

In both scenarios, the generation of microturbine, diesel generator, SOFC, PV1 and PV2 are assumed to be 18, 10, 7, 9 and 2.7 kW respectively. The dependency of output power of PV to temperature and irradiance is modeled and temperature and irradiance are assumed as 23 °C and 900 W/m^2 respectively.

The nominal and overloading characteristics of the BESS for charge and discharge are given in Tables 2 and 3 respectively [32]. With respect to the values of SOCmax and SOCmin of the BESS, in order to preserve 40% of the BESS capacity for charge/discharge

Table 1
Load-generation and exchange power of the MG.

Scenario of uncontrolled islanding	P_D (kW)	P_G (kW)	Exchange power (mismatch power) (kW)
Surplus	31.6	46.7	14.7
Shortage	66.0	46.7	20

Table 2
Nominal characteristic of the BESS.

Nominal capacity (Ah)	Max. constant current (A)	SOCmax (%)	SOCmin (%)
160	160	100	20

Table 3
Overloading characteristics of the BESS.

In discharge mode (generator action)		In charging mode (load action)	
Overloading coefficient P_{ov}	Permissible overloading duration (s)	Overloading coefficient P_{ov}	Permissible overloading duration (s)
$P_{ov} < 10$	5	$P_{ov} < 5$	5
$P_{ov} < 8$	15	$P_{ov} < 4$	15
$P_{ov} < 5$	60	$P_{ov} < 2$	60

Table 4
Characteristics of the designed BESS.

Scenario of uncontrolled islanding	Required overloading for BESS (kW)	Permissible overloading duration (s)	Power rating of BESS (kW)
Surplus	14.7	15	3.67
Shortage	20	60	4

activities at the surplus/shortage situations, the set point of SOC is set to 60% (SOC-*ref* = 60%).

For optimal sizing the BESS to fulfill the requirement of primary frequency control of the MG first, the BESS is designed based on the islanding scenario with surplus generation in which the mismatch power of the MG is 14.7 kW. Based on Eq. (6) the required overloaded power for the BESS is determined as 14.7 kW. Proper permissible overloading duration and nominal power of the BESS are determined as follows:

Initially, maximum overloading coefficient ($P_{ov} = K_1^{ch} = 5$) with corresponding permissible overloading duration ($t_1^{ch} = 5$ s) are chosen for the BESS. By using Eq. (7), the nominal power rating of the BESS is evaluated as 2.94 kW. The designed BESS is implemented into the MG and by time domain frequency simulation the response of system frequency in the case of uncontrolled islanding with 14.7 kW surplus power is evaluated. It is found that the battery with such overloading characteristics (capacity and duration) is not able to capture and stabilize system frequency. It means that the permissible overloading duration of the BESS is not enough for capturing power balance and should be longer. For this purpose, a lower value of overloading coefficient ($P_{ov} = K_2^{ch} = 4$) is adopted from Table 2 with the corresponding permissible overloading duration as $t_1^{ch} = 5$ s. For this design, simulation study shows that the overloaded power with the corresponding permissible duration is able to capture and stabilize system frequency. The nominal power of the BESS evaluated by equation 7 is 3.67 kW which is shown in Table 4.

Secondly, the shortage scenario is examined in which according to the maximum shortage generation of the MG, the required overloaded power (discharging) of the BESS is chosen as 20 kW. First, maximum overloading coefficient and corresponding minimum permissible overloading duration are adopted from Table 2 as $K_i^{ch} = 10, t_i^{dch} = 5$ s. The same process as the surplus scenario is carried out and at the end of the process, the satisfactory overloading coefficient, permissible overloading duration and nominal power of the BESS are evaluated as 5, 60 s. and 4 kW respectively as shown in Table 4.

Comparison of the two size obtained for the BESS based on the surplus and shortage scenarios, shows that the BESS designed the by shortage scenario is able to properly capture system frequency in the case of surplus situation. However, the BESS designed based on the surplus scenario is not able to stabilize system frequency for the shortage scenario. Therefore, the power rating 4 kW obtained based on the shortage scenario is adopted as the optimal size for the BESS.

Obviously if it was supposed to restore mismatch power of the MG by the nominal power of the BESS, a power rating of 20 kW was required.

Figs. 8–11 show frequency response of the MG and power output of the optimal BESS besides output of other microsources for both surplus and shortage scenarios respectively. As it can be seen, contribution of the BESS compared to other microsources is much bigger and faster such that it is able to quickly restore load-generation balance. After stabilizing frequency by the BESS, contributions of other microsources based on their droop characteristic come into play and consequently cause BESS to decrease its output power to zero for being ready for primary frequency control in the case of any new event.

Figs. 12 and 13 show variation in SOC of the BESS during frequency control for both surplus and shortage scenarios respectively. As it can be seen for the task of primary frequency control only a few percent (2–3%) of the SOC of the BESS has changed due to its contribution for initial restoration of the load-generation balance.

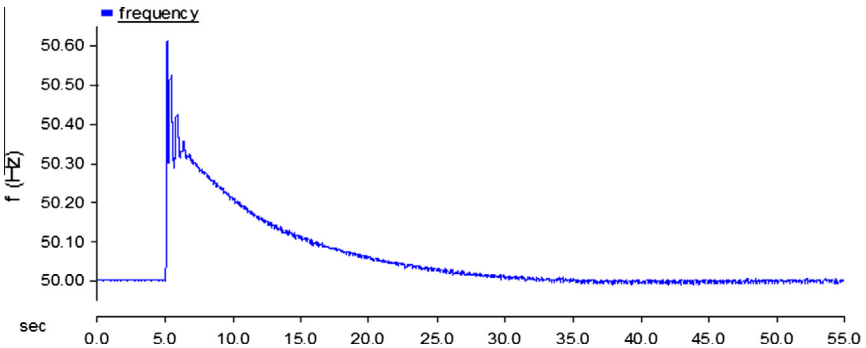

Fig. 8. Frequency behavior of the MG due to the BESS (surplus scenario).

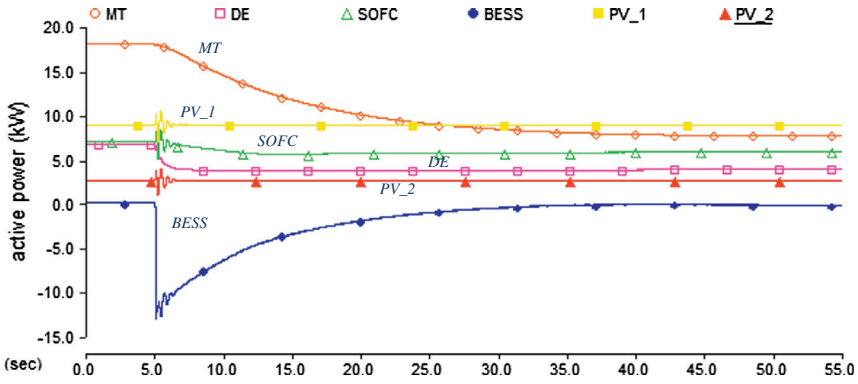

Fig. 9. Active power output of the BESS besides all microsources (surplus scenario).

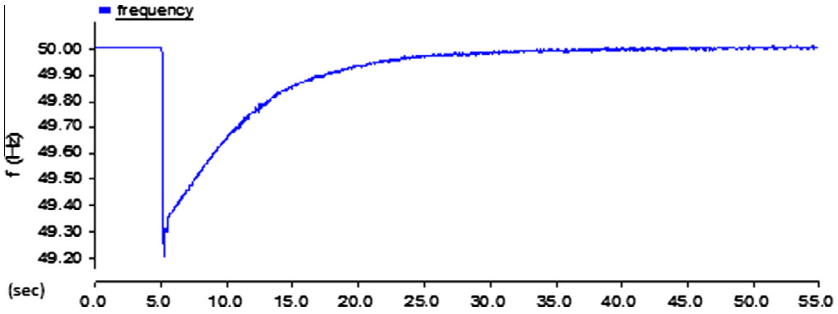

Fig. 10. Frequency behavior of the MG due to the BESS (shortage scenario).

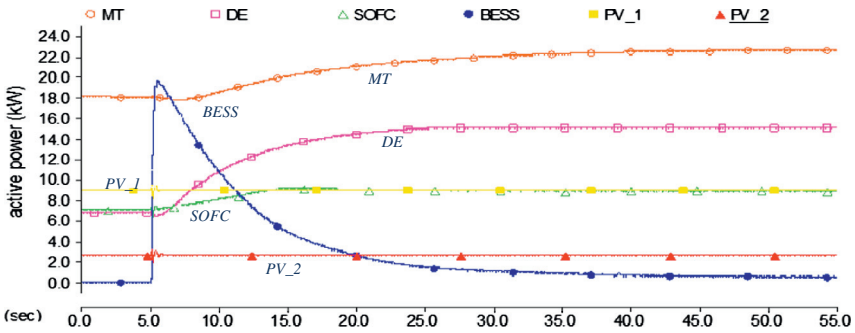

Fig. 11. Active power output of the BESS besides all microsources (shortage scenario).

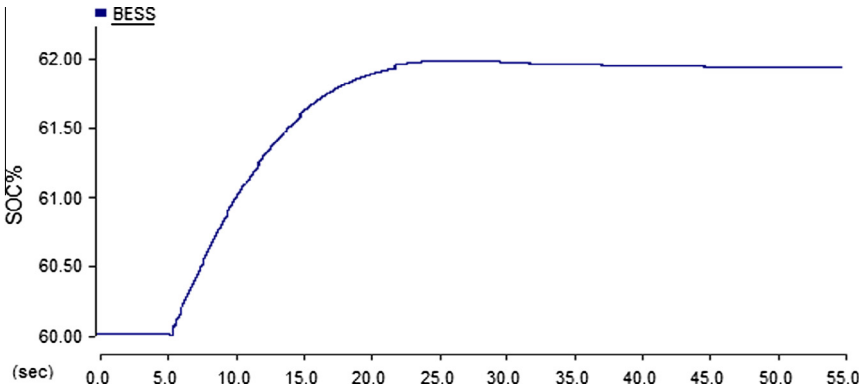

Fig. 12. Increase in SOC of the BESS during frequency control (surplus scenario).

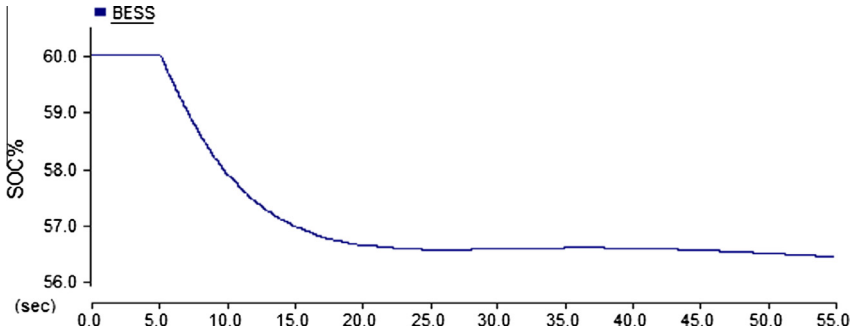

Fig. 13. Decrease in SOC of the BESS during frequency control (shortage scenario).

8. Conclusion

In this paper, a new approach is proposed for optimal sizing of the BESS for performing the task of primary frequency control in a Microgrid. The most significant contribution of the proposed approach which makes it different from other works is implementation of short term overloading characteristic of the BESS into primary frequency control. In fact, relying on the overloading characteristics of the BESS provided an opportunity for utilization of the overloading capacity of the BESS in a short time for fast injecting or absorbing power to the MG for restoration of load-generation balance. The simulation results demonstrated that utilization of the overloading characteristic of the battery enable a low size BESS capable to quickly response to power mismatch. The results showed that with respect to a mismatch power in the MG, a BESS with an optimal size of only 20% of the mismatch power which is designed by the proposed approach is capable for restoring load-generation power at the stage of the primary frequency control. Also, participation of the proposed BESS in the primary frequency control utilized only a few percent (2–4%) of the SOC of the BESS. Therefore, utilization of the overloading feature of the BESS for the primary frequency control appears to be very efficient and only a few percent of the BESS capacity including its power rating and SOC has been occupied. Optimal sizing of the BESS is determined based on the severe islanding scenario which is corresponding to the maximum of surplus/shortage of generation. Although, the control scheme and the optimal size of the BESS which are designed for primary frequency control of the MG are based on islanding scenarios, but the designed BESS will be able to participate in the primary frequency control of the islanded operation of the MG following any kind of disturbances. In the long term energy management activity of a MG in which a BESS may be used for energy exchange, it can participate in primary frequency control by allocating a few percent of its capacity for frequency control. Application of the proposed approach on a test system with promising results demonstrated its effectiveness.

References

[1] Llaria A, Curea O, Jiménez J, Camblong H. Survey on MGs: unplanned islanding and related inverter control techniques. Renew Energy 2011;36(8):1–10.
[2] Hatziargyriou ND, Meliopoulos APS. Distributed energy sources: technical challenges. IEEE Power Eng Soc Winter Meet 2002;2:1017–22.
[3] Smallwood CL. Distributed generation in autonomous and non-autonomous MG. In: Proc, 2002 IEEE rural elect. power conf; 2002. p. D1-1–D1-6.
[4] Tsikalakis A, Hatzargyriou N. Centralized control for optimizing MGs operation. IEEE Trans Energy Convers 2008;23(1):241–8. Mar.
[5] Tan Xingguo, Li Qingmin, Wanga Hui. Advances and trends of energy storage technology in Microgrid. Electr Power Energy Syst 2013;44:179–91.
[6] Pogaku N, Prodanovic M, Green Timothy C. Modeling, analysis and testing of autonomous operation of an inverter-based MG. IEEE Trans Power Electr 2007;22(2):613–25.
[7] Mehrizi-Sani A, Iravani R. Potential-function based control of a MG in islanded and grid-connected modes. IEEE Trans Power Syst 2010:1–8. pp. 99.
[8] Shahabi M, Haghifam MR, Mohamadian M, Nabavi-Niaki SA. MG dynamic performance improvement using a doubly fed induction wind generator. IEEE Trans Energy Convers 2009;24(1):137–45.
[9] Lidula NWA, Rajapakse AD. MGs research: a review of experimental MGs and test systems. Renew Sust Energy Rev 2011;15(1):186–202.
[10] El-Khattam W, Salama MMA. Distributed generation technologies, definitions and benefits. Electr Power Syst Res 2004;71(2):119–28.
[11] Jiayi, Chuanwen J, Rong X. A review on distributed energy resources and MG. Renew Sust Energy Rev 2007;12(9):2472–83.
[12] Dell RM, Rand DAJ. Energy storage – a key technology for global energy sustainability. J Power Sources 2001;100(1–2):2–17.
[13] Bando S, Sasaki Y, Asano H, Tagami S. Balancing control method of a MG with intermittent renewable energy generators and small battery storage. In: Proceedings of the IEEE PES general meeting – conversion and delivery of electrical energy in the 21st century; 2008. p. 1–6.
[14] Carrasco JM, Franquelo LG, Bialasiewicz JT, Galván E, Guisado RCP, Prats ḾAM, et al. Power-electronic systems for the grid integration of renewable energy sources: a survey. IEEE Trans Ind Electron 2006;53:1002–16.
[15] Kim AR, Seo HR, Kim GH, Park MW, Yu IK, Otsuki Y, et al. Operating characteristic analysis of HTS SMES for frequency stabilization of dispersed power generation system. IEEE Trans Appl Supercond Jun. 2010;20(3):1334–8.
[16] Kim JY, Jeon JH, Kim S-K, Cho C, Ho Park J, Kim HM, et al. Cooperative control strategy of energy storage system and microsources for stabilizing the mg during islanded operation. IEEE Trans Power Electron Soc 2010;25(12):3037–48.
[17] Hatziargyriou H, Kanellos F, Kariniotakis G, Le Pivert X, Jenkins N, Jayawarna N, et al. Modeling of micro-sources for security studies, presented at CIGRE Session France; 2004.
[18] Mercier P, Cherkaoui R, Oudalov A. Optimizing a battery energy storage system for frequency control application in an isolated power system. IEEE Trans Power Syst 2009;24(3).
[19] Oudalov A, Chartouni D, Ohler C, Linhofer G. Value analysis of battery energy storage applications in power systems. In: Proc. 2nd IEEE PES power systems conf. expo., Atlanta, GA; 2006. p. 2206–11.
[20] Sulzberger VT, Zeinoski I. The potential for application of energy storage capacity on electrical utility systems in the United States part I. IEEE Trans Power Appl Syst 1976;PAS-95(11).
[21] Lu CF, Liu C-C, Wu C-J. Dynamic modelling of battery energy storage system and application to power system stability. IET Proc Gener Transm Distrib 1995;142(4):429–35.
[22] Aditya SK, Das D. Application of battery energy storage system to load frequency control of an isolated power system. Int J Energy Res 1999;23:247–58.
[23] Oudalov A, Chartouni D, Ohler C. Optimizing a battery energy storage system for primary frequency control. IEEE Trans Power Syst 2007;22(3):1259–66.
[24] Aditya SK, Das D. Application of battery energy storage system to load frequency control of an isolated power system. Int J Energy Res 1999;23:247–58.
[25] Zhu Y, Tomsovic K. Development of models for analyzing the load-following performance of microturbines and fuel cells. Electr Power Syst Res 2002;62(1):1–11.
[26] Frirdel V. Modeling and simulation of a hybrid wind-diesel MG. MSc thesis. School of Electrical Engineering, Royal Institute of Technology, Stockholm, Sweden, June 2009.
[27] Pogaku N, Prodanovic M, Green TC. Modeling, analysis and testing of autonomous operation of an inverter-based MG. IEEE Trans Power Electr 2007;22(2):613–25.
[28] Katiraei F, Iravani MR. Power management strategies for a MG with multiple distributed generation units. IEEE Trans Power Syst 2006;21(4):1821–31.
[29] Xiangjun Li, Dong Hui, Li Wu, Xiaokang Li. Control strategy of battery state of charge for wind/battery hybrid power system. In: IEEE international symposium on industrial electronics (ISIE), 4–7 July 2010.
[30] He Zhi-Wei, Gao M, Xu Jie. EKF-Ah based state of charge online estimation for lithium-ion power battery. In: International conference on computational intelligence and security CIS; 2009.
[31] Thounthong Phatiphat. Control of fuel cell/battery hybrid source for electric vehicle applications. ECTI Trans Electr Eng Electron Commun 2007;5(2).
[32] "Lithium Iron Phosphate Battery", $LiFePO_4$ battery specification. Hipower New Energy Group Co., Ltd., <www.hipowergroup.com>; 2010.